Fractional Synchronization of Spin-Torque Nano-Oscillators

Sergei Urazhdin and Phillip Tabor

Department of Physics, West Virginia University, Morgantown, West Virginia 26506, USA

Vasil Tiberkevich and Andrei Slavin

Department of Physics, Oakland University, Rochester, Michigan 48309, USA
(Received 14 June 2010; published 31 August 2010)

We experimentally demonstrate a series of fractional synchronization regimes (Devil's staircase) in a spin-torque nano-oscillator driven by a microwave field. These regimes are characterized by rational relations between the driving frequency and the frequency of the oscillation. An analysis based on the phase model of auto-oscillator indicates that fractional synchronization becomes possible when the driving signal breaks the symmetry of the oscillation, while the synchronization ranges are determined by the geometry of the oscillation orbit. Measurements of fractional synchronization can be utilized to obtain information about the oscillation characteristics in nanoscale systems not accessible to direct imaging techniques.

Downscaling of electronic devices requires ever increasing operating current densities. The out-of-equilibrium state produced by large currents can lead to new phenomena, providing unique opportunities for novel device architectures. In particular, high current densities in nanoscale magnetic devices result in large-amplitude magnetization oscillations, forming the basis for a novel type of nanoscale microwave oscillator, the spin-torque nano-oscillator (STNO) [1–4]. STNO is not only one of the smallest known auto-oscillators, but also a complex non-linear dynamical system whose frequency is dependent on the amplitude of the oscillation, due to the dependence of the demagnetizing fields on the oscillation trajectory.

The nonlinearity of STNO allows one to tune the generation frequency by electric current, and also enhances its ability to synchronize to periodic external signals [5], providing a potential route for enhancing the oscillation characteristics by mutual synchronization in arrays of STNO. Following this approach, synchronization of two [6,7] and even four [8] STNO with similar frequencies has been recently observed experimentally.

All the previous experiments on the STNO synchronization utilized a driving signal provided by a *microwave current* whose frequency f_e was close to the STNO oscillation frequency f_0 [9–11]. In this Letter, we utilize a driving signal provided by a *microwave field* to experimentally demonstrate that the complex nonlinear oscillation characteristics of STNO lead to a large class of synchronization phenomena observed not only for f_e close to f_0, but also when their ratio $r = f_e/f_0$ is close to integer or certain rational numbers. We also show theoretically that these synchronization phenomena provide important information about the properties of the oscillation.

We used *e*-beam lithography to fabricate devices with structure Cu(40)Py(15)Cu(8)Py(3.5)Cu(60), where thicknesses are in nm and Py $= \mathrm{Ni_{80}Fe_{20}}$. The free Py(3.5) layer

was patterned into a 100 nm $\times$ 50 nm nanopillar, while the polarizing Py(15) layer was left extended with dimensions of several micrometers. Magnetic oscillations of the nanopillar were induced by a dc bias current $I_0 > 0$ flowing from the polarizer to the free layer. The microwave driving field h_e was generated by a 300 nm $\times$ 250 nm Cu microstrip antenna fabricated on top of the nanopillar. It was oriented at 45° with respect to the nanopillar easy axis, and electrically isolated from STNO by a $\mathrm{SiO_2}(50)$ layer. The Oersted field produced by the microstrip was calibrated by comparing the dependence of f_0 on the bias field H_0 to its dependence on the dc current applied to the microstrip. By applying a microwave current to the microstrip, microwave fields of up to $h_e = 30$ Oe were generated at the location of STNO without noticeable heating. Our technique enabled spectroscopic measurements at arbitrary relations between the driving and the oscillation frequencies, and provided strong driving essential for the observation of the phenomena described below. The parasitic coupling between the microstrip and the STNO was less than -20 dB, resulting in induced microwave currents that did not exceed 40 μA. The bias field was $H_0 = 350$ Oe unless specified otherwise, applied in-plane perpendicular to the microstrip. All measurements were performed at 5 K. The reported behaviors were confirmed for three devices.

The characterization of STNO was performed by measurements of auto-oscillation spectra. The peaks exhibited a typical full width at half maximum (FWHM) of 5 MHz and Lorentzian line shape characteristic of thermal broadening [Fig. 1(a)] [12,13]. The oscillation frequency increased with increasing H_0, and decreased with increasing I_0 [Fig. 1(b)], consistent with the established properties of similar STNOs [3].

In spectroscopic measurements of oscillation at finite driving field h_e, the oscillation frequency f_0' remained close to the free-running frequency $f_0 = 2.94$ GHz for
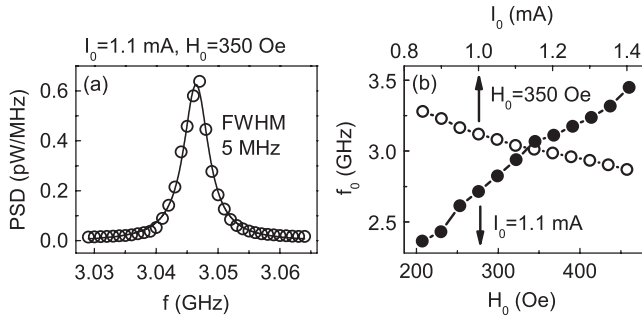
FIG. 1. Free-running oscillation characteristics of STNO. (a) Circles: a typical oscillation spectrum. Curve: Lorentzian fit. (b) oscillation frequency vs bias field (solid symbols and bottom scale), and vs bias current (open symbols and top scale).

most of the values of the driving frequency f_e, with the exception of the regions where the ratio $r = f_e/f_0$ is close to all integer ($r = 1, 2, 3, 4$) and several rational ($r = 3/2$, $7/3, 5/2, 7/2$) values (Fig. 2). In these regions, f_0' follows a linear relationship with f_e, as expected for the synchronized oscillation. Since the spectroscopic peaks observed at $r = 1$ are dominated by the parasitic coupling to the driving signal, in this regime the synchronization can be identified by the breaks in the $f_0' \approx$ const line. In contrast, spectroscopic measurements of all the other synchronization regimes were performed *below* the driving frequency, eliminating the effects of parasitic signals on the spectra, and enabling us to directly determine the characteristics of the synchronized oscillations.

An example of spectroscopic measurements for one of these regimes ($r = 2$) is shown in Fig. 3(a). The synchronized oscillation peaks become significantly narrower and their maximum spectral amplitude dramatically increases, while the oscillation frequency follows an exact relationship $f_0'/f_e = 2$ within the measurement precision of better than 0.05% [Fig. 3(b)]. To enable a wide frequency scan
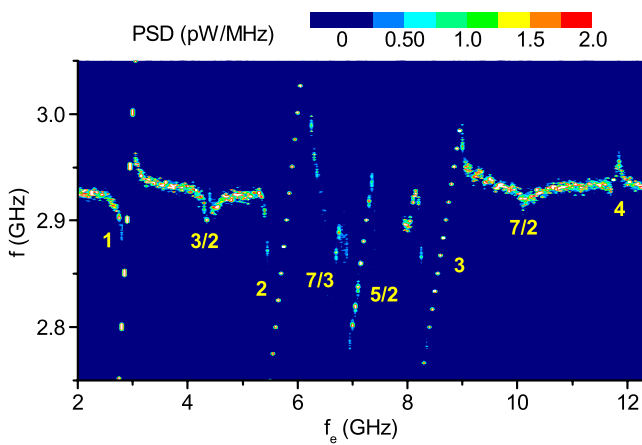

FIG. 2 (color online). Dependence of the oscillation spectra on the driving frequency, at $h_e = 13$ Oe and $I_0 = 1.3$ mA. The scale indicates the power spectral density (PSD) of the spectral signal. The values of $r = f_e/f_0'$ for the identified synchronization regimes are labeled.

shown in Fig. 3(a), these measurements were performed with a bandpass of 300 kHz that exceeded the width of the synchronized peak. Separate measurements at our setup's ultimate resolution of 1 kHz showed that synchronization resulted in an increase of the maximum spectral amplitude by three orders of magnitude Fig. 3(c), and a similar magnitude of decrease of FWHM to the smallest value of 1.4 kHz [Fig. 3(d)]. These results demonstrate that the oscillator becomes fully phase locked with the driving signal for at least 1 ms (3×10^6 oscillation cycles) without a single phase slip. We note that the total power generated by STNO is determined by the amplitude of the magnetization oscillation, which is not significantly affected by the driving field. Indeed, the increase of the peak amplitude is compensated by the decrease of the linewidth, so that the total generated power remains approximately constant.

To quantitatively characterize the synchronization, we define the synchronization interval $\Delta f_r = (f_{e,\max} - f_{e,\min})/r$, where $f_{e,\max}$ ($f_{e,\min}$) is the maximum (minimum) driving frequency at which the synchronization is observed. Although both the integer interval Δf_2 and the fractional interval $\Delta f_{5/2}$ increase with the driving amplitude, the value of Δf_2 depends linearly on h_e, while the dependence of $\Delta f_{5/2}$ on h_e is strongly nonlinear [Fig. 4(a)]. Integer synchronization persisted at the smallest driving signal $h_e = 1.3$ Oe used in our measurements, while the $r = 5/2$ synchronization disappeared at $h_e < 4$ Oe, demonstrating that strong driving provided by our technique is essential for the observation of fractional synchronization. The value of Δf_2 increases at small I_0, exceeding 1 GHz at $I_0 < 0.9$ mA. In contrast, $\Delta f_{5/2}$ decreases at small I_0, vanishing at $I_0 < 0.9$ mA [Fig. 4(b)].

The complexity of the observed synchronization patterns suggests that they contain intricate information about
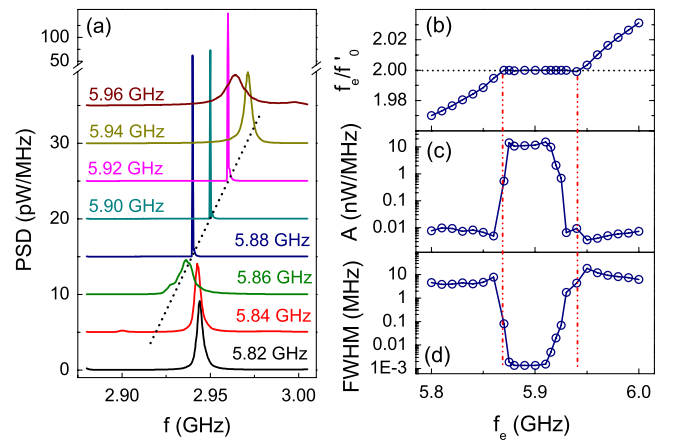

FIG. 3 (color online). The $r = 2$ synchronization at $I_0 = 1.3$ mA, $h_e = 2$ Oe. (a) Oscillation spectra at the labeled values of f_e, acquired with a bandpass of 300 kHz. Dotted line indicates $f = f_e/2$. (b)–(d) Characteristics of the oscillation peaks acquired with a bandpass of 1 kHz: (c) the ratio of f_e to f_0', (c) the peak spectral amplitude A, (d) FWHM of the oscillation peak. Dashed lines show the synchronization boundaries.
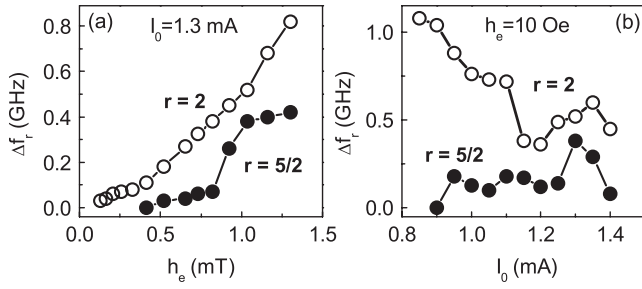
FIG. 4. Dependence of the integer synchronization interval Δf_2 (open symbols) and fractional interval $\Delta f_{5/2}$ (solid symbols) on h_e (a), and on I_0 (b).

the oscillator. To analyze the mechanisms of synchronization, we consider the classic model describing the state of the oscillator only by the phase ϕ defined to increase linearly with time in the autonomous regime [14,15]. Under the influence of a periodic driving signal, the dynamics can be described by

$$d\phi/dt = \omega_0 + \mu \, \mathrm{Re}[g(\phi)e^{-i\omega_e t}] \qquad (1)$$

Here, μ is the amplitude of the driving force, $\omega_{0,e} = 2\pi f_{0,e}$, and the complex function $g(\phi)$ determined by the geometry of the oscillation trajectory and the driving signal describes the position-dependent sensitivity of the oscillator to the driving force. Since $g(\phi)$ is periodic, it can be expressed as $g(\phi) = \sum_n g_n e^{in\phi}$, where the Fourier components g_n contain the information about the oscillation trajectory.

To determine the relation of the function $g(\phi)$ to synchronization, we consider a fractional synchronized state $r = p/q$, where p and q are mutually simple integers. The oscillator completes q cycles during p periods of the driving force;, i.e., its phase satisfies $\phi(t + p/f_e) = \phi(t) + 2\pi q$. Expanding it into a Fourier series, $\phi(t) = \phi(0) + \omega_e t q/p + \sum_{k \neq 0} \phi_k e^{-i\omega_e t/p}$ and inserting into Eq. (1), we obtain an equation for ϕ_k which can be solved iteratively in powers of μ. The condition of solvability of this equation determines the synchronization interval $\Delta\omega_r$.

To the first order in μ, only the synchronization at integer $r = p/1$ is possible, with the interval

$$\Delta\omega_p \approx 2\mu|g_p|. \qquad (2)$$

Fractional synchronization ($q > 1$) appears only in the higher orders in μ, with intervals $\Delta\omega_r \propto (\mu g_p)^q$. In particular, for $r = p/2$

$$\Delta\omega_{p/2} \approx \frac{\mu^2}{\omega_0} \left| \sum_n g_n g_{p-n} \right|. \qquad (3)$$

The linear dependence of $\Delta\omega_p$ on $\mu \propto h_e$, and the nonlinear dependence of $\Delta\omega_{p/2}$ are in agreement with Fig. 4(a).

It is generally difficult to calculate the function $g(\phi)$ that determines the synchronization intervals, since it depends *both* on the form of the driving signal and the oscillation

trajectory. However, it is possible to experimentally determine each component g_p by measuring the corresponding synchronization intervals [Eq. (2)]. Moreover, symmetry analysis described below enables one to determine the general conditions for the existence of specific synchronization regimes, providing a qualitative insight into the mechanism of fractional synchronization.

The oscillation trajectory of STNO is approximately symmetric with respect to a half-period rotation $\phi \to \phi + \pi$ [3]. A microwave field parallel to the oscillation symmetry axis **s** produces a symmetric driving force; i.e., a π phase shift of the driving signal does not change the oscillation phase. In this case, all the odd Fourier components of $g(\phi)$ vanish, $g_{2n+1} = 0$, and only even integer synchronization regimes can be observed. On the other hand, $\mathbf{h}_e \perp \mathbf{s}$ produces an antisymmetric driving force. In this case, all the even components of $g(\phi)$ vanish, $g_{2n} = 0$, and only odd integer synchronization regimes can be observed.

To understand the implications of our symmetry analysis for fractional synchronization, we consider the half-integer regime [Eq. (3)]. Since the numbers p and $q = 2$ are mutually simple, p is odd. Therefore, the indices of the Fourier components g_n and g_{p-n} in Eq. (3) have different parity. Since the even spectral components describe perturbations that are symmetric with respect to a half-period rotation, and the odd ones describe antisymmetric perturbations, the $q = 2$ fractional synchronization of a symmetric auto oscillator is possible *only* if the driving signal contains both symmetric and antisymmetric components, or in other words, if the signal breaks the symmetry of the oscillator. In our experiment, $\mathbf{h}_e$ was parallel to $\mathbf{H}_0$, at 45° with respect to the nanopillar axis. Modeling shows that, as a result of the demagnetizing effects, **s** was rotated by 20° with respect to $\mathbf{h}_e$, creating the symmetry-breaking geometry necessary for the fractional synchronization.

To confirm the results of our analysis, we performed numerical simulations of STNO synchronization to a microwave field (Fig. 5). The temporal evolution of magnetization was determined by integration of the Landau-Lifshitz equation within a macrospin approximation, which included the spin-torque and the driving field terms, with the parameter values corresponding to the experimental conditions of Fig. 2: $H_0 = 350$ Oe oriented at 45° with the nanopillar easy axis, $I_0 = 1.3$ mA, $h_e = 13$ Oe, saturation magnetization $M_s = 640$ G, easy-axis anisotropy field $H_a = 200$ Oe, Gilbert damping constant $\alpha = 0.01$, and dimensionless spin-polarization efficiency $\eta = 0.18$. The spectral characteristics of the driven oscillation were determined by Fourier transformation of the simulated dynamics.

In agreement with our symmetry analysis, only the even integer synchronization regimes are prominent for $\mathbf{h}_e \parallel \mathbf{s}$ [Fig. 5(a)], and only the odd integer synchronization regimes are prominent for $\mathbf{h}_e \perp \mathbf{s}$ [Fig. 5(a)]. In both cases, small but finite fractional synchronization ranges are
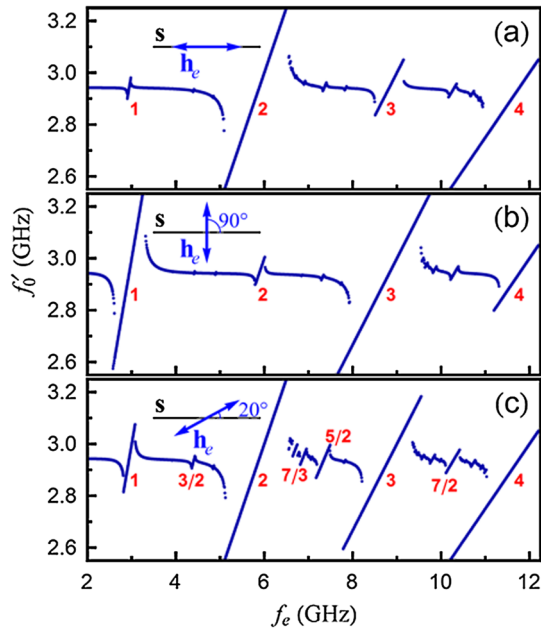
FIG. 5 (color online). Simulated dependence of f_0' on f_e, for different orientations of $\mathbf{h}_e$ with respect to $\mathbf{s}$: (a) $\mathbf{h}_e \parallel \mathbf{s}$, (b) $\mathbf{h}_e \perp \mathbf{s}$, and (c) angle of 20° between $\mathbf{h}_e$ and $\mathbf{s}$ corresponding to the experimental configuration. Prominent synchronization regimes are labeled.

caused by the slight asymmetry of the oscillation trajectory. On the other hand, simulation of the experimental configuration $\mathbf{h}_e \parallel \mathbf{H}_0$ [Fig. 5(c)], corresponding to an angle of 20° between $\mathbf{h}_e$ and $\mathbf{s}$, produces large integer and fractional synchronization ranges, in excellent semi-quantitative agreement with the data (Fig. 2). Additional simulations for $f_e < f_0$ showed that fractional synchronization to symmetry-breaking perturbations is also possible at $r < 1$.

Our symmetry analysis is equally applicable to synchronization by microwave current. In this case, the symmetry of the driving force is determined by the direction of the current polarization. In the published measurements of the main synchronization regime $r = 1$ [9–11], the current polarization was nearly parallel to $\mathbf{s}$, and consequently the driving force was approximately symmetric. Since synchronization with $r = 1$ requires antisymmetric perturbation [see Eq. (2)], our analysis explains why a large magnitude of the driving current comparable to I_0 was required in these measurements. In contrast, a significantly more efficient $r = 2$ synchronization can be expected in this geometry.

In conclusion, we have experimentally demonstrated synchronization of a spin torque nano-oscillator at fractional ratios between the frequency of the driving microwave field and the frequency of the oscillation. The phenomenon of fractional synchronization opens new routes for efficient synchronization of auto-oscillators whose frequencies are not close to each other, and for the development of novel nanoscale signal processing devices

such as microwave frequency converters. We developed a general model of synchronization, which shows that fractional synchronization of symmetric oscillators becomes possible only if the driving force breaks the oscillation symmetry, and more generally, that the efficiency of synchronization in any regime is determined by the symmetry of the driving signal. Fractional synchronization for a controlled symmetry of the driving signal represents a novel tool for the characterization of auto-oscillators. For instance, one can determine the orientation of the precession axis by measuring the dependence of the synchronization intervals on the direction of the driving field. This characterization technique is especially important for the nanoscale oscillators such as STNO, which are not accessible to the standard imaging and characterization techniques.

[1] J. Slonczewski, J. Magn. Magn. Mater. **159**, L1 (1996).

[2] L. Berger, Phys. Rev. B **54**, 9353 (1996).

[3] S. I. Kiselev, J. C. Sankey, I. N. Krivorotov, N. C. Emley, R. J. Schoelkopf, R. A. Buhrman, and D. C. Ralph, Nature (London) **425**, 380 (2003).

[4] W. H. Rippard, M. R. Pufall, S. Kaka, S. E. Russek, and T. J. Silva, Phys. Rev. Lett. **92**, 027201 (2004).

[5] A. Slavin and V. Tiberkevich, IEEE Trans. Magn. **45**, 1875 (2009).

[6] S. Kaka, M. R. Pufall, W. H. Rippard, T. J. Silva, S. E. Russek, and J. A. Katine, Nature (London) **437**, 389 (2005).

[7] F. B. Mancoff, N. D. Rizzo, B. N. Engel, and S. Tehrani, Nature (London) **437**, 393 (2005).

[8] A. Ruotolo, V. Cros, B. Georges, A. Dussaux, J. Grollier, C. Deranlot, R. Guillemet, K. Bouzehouane, S. Fusil, and A. Fert, Nature Nanotech. **4**, 528 (2009).

[9] W. H. Rippard, M. R. Pufall, S. Kaka, T. J. Silva, S. E. Russek, and J. A. Katine, Phys. Rev. Lett. **95**, 067203 (2005).

[10] B. Georges, J. Grollier, M. Darques, V. Cros, C. Deranlot, B. Marcilhac, G. Faini, and A. Fert, Phys. Rev. Lett. **101**, 017201 (2008).

[11] J. C. Sankey, P. M. Braganca, A. G. F. Garcia, I. N. Krivorotov, R. A. Buhrman, and D. C. Ralph, Phys. Rev. Lett. **96**, 227601 (2006).

[12] J. C. Sankey, I. N. Krivorotov, S. I. Kiselev, P. M. Braganca, N. C. Emley, R. A. Buhrman, and D. C. Ralph, Phys. Rev. B **72**, 224427 (2005).

[13] V. S. Tiberkevich, A. N. Slavin, and Joo-Von Kim, Phys. Rev. B **78**, 092401 (2008).

[14] R. Adler, Proc. IRE **34**, 351 (1946).

[15] A. Pikovsky, M. Rosenbblum, and J. Kurths, *Synchronization: A Universal Concept in Nonlinear Sciences* (Cambridge, New York, 2001).